Journal of Fluorescence (2019) 29:101–110
https://doi.org/10.1007/s10895-018-2314-4

ORIGINAL ARTICLE

Multispectroscopic and Computational Investigation of *ct*-DNA Binding Properties with Hydroxybenzylidene Containing Tetrahydrocarbazole Derivative

Sule Ozkan[1] · Tugba Taskin-Tok[2] · Ayse Uzgoren-Baran[3] · Nuriye Akbay[4]

Received: 8 August 2018 / Accepted: 15 October 2018 / Published online: 25 October 2018

Abstract

Mode of interaction of a new tetrahydrocarbazole derivative with *ct*-DNA has been investigated systematically using fluorescence spectroscopy, UV-Vis spectroscopy and circular dichroism spectroscopy. It is concluded that TAH could intercalate into the base pairs of *ct*-DNA, and the fluorescence quenching by *ct*-DNA was static quenching type. Beside the multispectroscopic results, computational studies were done. Molecular docking results revealed that the TAH-DNAs complexes might be classified as druggable molecule in drug design. Additionally, DNA binding studies exhibited that TAH complexes have different interaction and orientation abilities to each DNA isomer. Combination of experimental and computational data showed that reported TAH is promising structure and deserves further applications.

Keywords Fluorescence · *ct*-DNA · Tetrahydrocabazoles · Stern-Volmer · Groove binding

Introduction

DNA is the best cellular target for many natural and synthetic organic molecules, particularly potential anticancer and antiviral drugs [1–4]. Despite the all attention to develop tumor cell targeted drugs, most of the anticancer chemotherapeutic drugs are DNA damaging agents. The clarifying the chemical interaction types of small molecules with DNA is important for giving notice their therapeutic probable and designing new and low toxical drugs for clinical usage. Interaction of small molecules with double stranded DNA can be characterized by three general binding modes: intercalation, groove binding and covalent binding [5–8]. Intecalators are generally planar aromatic molecules and interact with DNA by inserting their planar chromophores between adjacent DNA base pairs [9]. Groove binders are generally crescent shaped, cationic ligands interact with *ds*-DNA by fixation in its groove. Both of these weak interactions are further stabilized by number non-bonding interactions such as van der Waals forces, hydrophobic forces, ionic forces and hydrogen bonds. Most drugs tend to interact non-covalently with DNA through two general modes, groove binding and intercalation [10].

Tetrahydrocabazoles are well known core-structure of naturally occurring carbazole alkaloids and also core structure of some FDA approved drugs such as ondansetron, frovatriptan and Ramatroban [11]. As known that tetrahydrocarbazole compounds have a large place of biological activities such as antibacterial [12], cytotoxic activity against human cancer cells [13] and anti-HPV activities [14]. In addition Schiff base-hydrazones are attractive targets for researchers worldwide in the fields of biology and medicinal chemistry because of their broad spectrum of activities. They denote antibacterial, antifungal [15], anticonvulsant [16], antiinflammatory [17], antimalarial [18] and antituberculosis activities [19]. Because of the variety of biological activities, scientists

Electronic supplementary material The online version of this article (https://doi.org/10.1007/s10895-018-2314-4) contains supplementary material, which is available to authorized users.

✉ Nuriye Akbay
nuriye.akbay@medeniyet.edu.tr

[1] Department of Chemistry, Namık Kemal University, 59030 Tekirdag, Turkey

[2] Department of Chemistry, Gaziantep University, 27310 Gaziantep, Turkey

[3] Department of Chemistry, Hacettepe University, Beytepe, 06800 Ankara, Turkey

[4] Department of Chemistry, Istanbul Medeniyet University, 34700 Istanbul, Turkey

pay attention tetrahydrocarbazole derivatives to plan, organize and improve newer approaches towards the discovery of new drugs. For the development of new drugs, it is the important step to understand functional mechanism of drug candidates with DNA.

In the light of the previous studies, we have synthesized a novel acyl hydrazine having tetrahydrocarbazole moiety as shown in the Scheme 1 and systematically studied its interaction with *ct*-DNA. We characterized the quenching, binding and thermodynamic constants and interaction mechanism of the studied system by fluorescence spectroscopy, UV-Vis absorption spectroscopy and circular dichroism (CD) spectroscopy. Additionally, interaction mechanism of TAH with *ct*-DNA at molecular level has been explored by molecular docking calculations. The results could provide contribution in designing new and effective drugs from tetrahydrocarbazoles.

Experimental and Computational Details

Syntheses and Characterizations of TAH

2.2 mmol Salicylaldehyde was added into the 2.2 mmol 2,3,4,9-tetrahydro-1*H*-carbazole-3-carbohydrazide in ethanol under continuous stirring and mixture was heated for 1.5 h. After the reaction completed, the solution was allowed to cool to the room temperature and after cooling ethanol was removed by rotary evaporator. Water washing was used to remove the impurities from residue and after filtration solid was dried to get the demanded product. The compound was purified by recrystallization using absolute ethanol.

N′-(2-hydroxybenzylidene)-2,3,4,9-tetrahydro-1H-carbazole-3-carbohydrazide (TAH) Pale yellow solid, yield 85%, mp 248–249 °C. IR (ν_{max}): 3401 (N-H), 3052 (C-H), 2926 (C-H), 2858 (C-H), 1668 (C=O), cm^{-1}. ^{1}H NMR (400 MHz, DMSO): δ = 1.93–1.96 (m, 1H, CH), 2.11–2.18 (m, 1H, CH), 2.72–2.95 (m, 4H), 3.51 (m, 1H, CH), 6.88–7.61 (m, 8H, ArH), 8.44 (8.34*, s, 1H, =CH), 10.75 (10.75*, s, 1H, NH_{indole}), 11.25 (10.17*, s, 1H, OH), 11.77 (11.33*, s, 1H, NH). APT-NMR (100 MHz, DMSO): δ = 22.6, 24.6, 26.5, 107.2, 111.1, 116.8, 117.6, 118.6, 119.1, 119.8, 120.7, 127.5, 129.9, 131.7, 134.1, 136.4, 147.2, 157.8.

Reagents

All chemicals were supplied from Sigma-Aldrich Chemical Co. The stock solution of TAH was prepared in DMSO as 2.0×10^{-3} mol/L. Calf thymus deoxyribonucleic acid (sodium salt of *ct*-DNA, Sigma) stock solution was prepared in Tris-HCl buffer solution at pH 8.0. Concentration of stock DNA solution was evaluated by the absorption values of solution at 260 nm (molar coefficient: 6600 M^{-1} cm^{-1}). To find out the purity of DNA the ratio of the absorbance values at 260 to at 280 nm were checked. Prepared ct-DNA solution gave a ratio of $A_{260}/A_{280} > 1.8$, which points that purity of DNA was enough for experimental studies. Daily prepared aqueous solutions by appropriate dilution from stock solutions were used in the experiments and all stock solutions were stored in refrigerator at 4 °C till use.

Apparatus

FS5-spectrofluoremeter (Edinburgh Instruments) was used in all fluorescence and UV-visible absorption measurements. Used spectrofluoremeter was equipped with a 150 W xenon lamp source and 1.0 cm quartz cell and the excitation and emission band pass slits were adjusted as 3.5 nm for all studies. Melting point of the compound was measured by electrothermal digital melting point apparatus in a sealed tube and is uncorrected. ^{1}H-NMR and APT spectra were recorded with Bruker DPX-400, 400 MHz High Performance Digital FT-NMR Spectrometer and DMSO-d_6 was used as solvent in all measurements. The chemical shifts were recorded in δ values (ppm). Chemical shifts (δ) of rotameric hydrogens whenever identified are shown within the parenthesis using giving an asterisk (*) along with that of the other form. Silicagel-coated aluminum sheets were used to check the purity of the compound by thin layer chromatography. IR spectra was recorded on a Thermo Scientific Nicolet iS10 spectrometer by using KBr pellets. CD spectra of *ct*-DNA and TAH-*ct*-DNA complex were recorded on a Jasco J-815 spectropolarimeter (Jasco Inc., UK) by using a quartz cell with a 0.1 cm path length in pH 7.4 PBS buffer. CD spectra of all samples were obtained from 220 to 320 nm with a scan speed of 100 nm min^{-1} at 298 K under constant nitrogen flush. Three scans were accumulated for each sample. The results were expressed as ellipticity (mdeg). pH measurements were carried out with Ohaus Starter 3100 pHmeter.

Scheme 1 Syntheses of TAH from tetrahydrocarbazole hydrazide

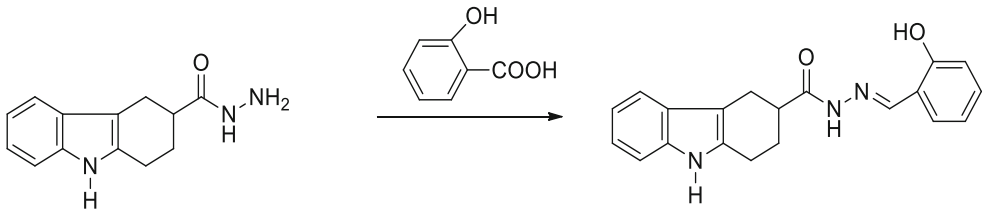

UV-Vis Absorption and Fluorescence Titrations

UV-Vis absorption measurements were performed by adding known aliquouts of *ct*-DNA to the solutions of TAH at a fixed concentration of 5.0×10^{-6} mol/L in 2.0 mL Tris-HCl buffer (pH 8.0). To perform the fluorescence titrations known quantities of *ct*-DNA were added into the TAH solution (5.0×10^{-6} mol/L) and the effect of *ct*-DNA on THA fluorescence were recorded. The effect of *ct*-DNA on tetrahydrocarbazole fluorescence was investigated at two different temperatures (25 and 37 °C) by fluorimetric titration. The fluorescence emission spectra of TAH were collected between 400 and 600 nm upon excitation at 360 nm. Dilution effect on fluorescence emission of dyes was eliminated by using the *ct*-DNA solution contained same amount dye in the titrations.

Docking Study

In this process, AutoDock 4.2 [20] was used to exert molecular docking for understanding interactions between TAH and each DNA isomer. The novel synthesized compound, TAH as ligand and DNAs including A-DNA (PDB: 3V9D) [21] and B-DNA (PDB: 1BNA) [22] forms were prepared using Gaussian09 (G09) [23] for molecular docking studies. The geometry and energy optimizations of the compound were computed at DFT/B3LYP/6-31G* level as implemented in G09. Their positions of DNAs were subsequently optimized using CHARMm force field and the adopted-basis Newton-Raphson (ABNR) method [24] available in the DS 2018 protocol [25] until the root mean square deviation (RMSD) gradient was <0.05 kcal/mol $Å^2$. AutoDock 4.2 was performed using Lamarckian genetic algorithm for all docking process. The default settings were used for all parameters. The best pose for the complexes was defined based on the binding energy and inhibition constant (Ki) values.

Results and Discussion

Fluorescence spectroscopy, especially the quenching effect of DNA on the fluorescence of small molecules is one of the most useful and common used technique to understand the interaction of the small organic molecules as potential drugs. Fluorescence quenching corresponds to any fluorescence intensity decreasing process of the investigated fluorophore upon addition a quencher. In the represented study we investigated the effect of *ct*-DNA on the fluorescence spectra of tetrahydrocarbazole derivative to characterize the interaction type of the compound with *ct*-DNA (Fig. 1). While the fluorescence intensity of TAH decreases with the increase of *ct*-DNA amount, maximum emission wavelength and the shape of the band stayed

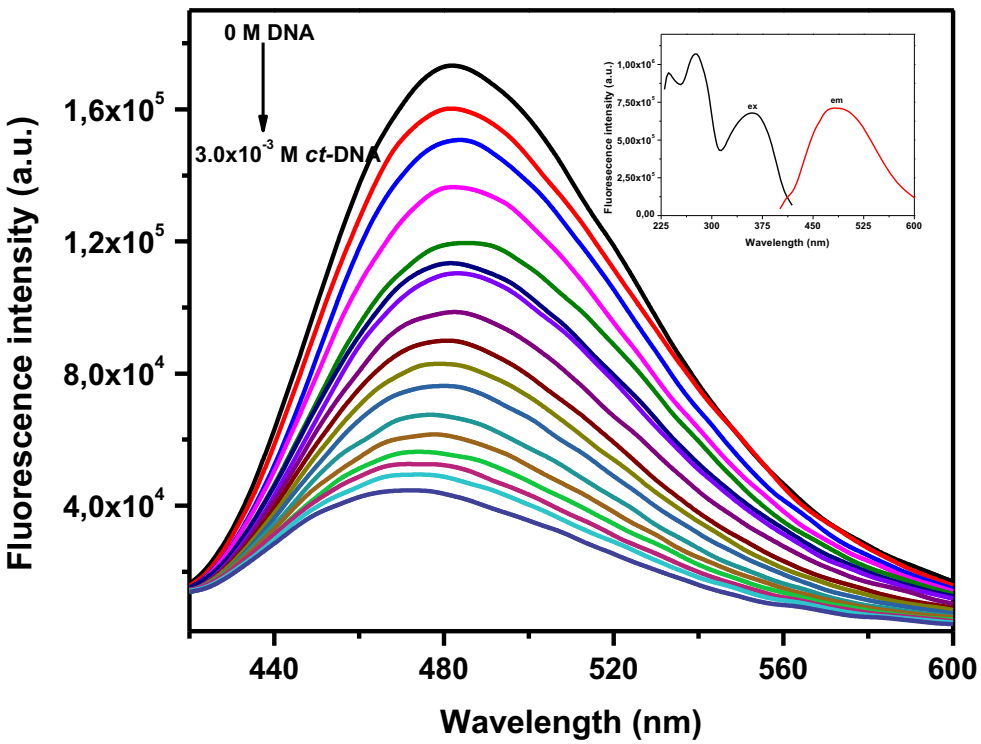

Fig. 1 *ct*-DNA effect on the fluorescence emission of TAH (λ_{ex} = 360 nm, $C_{ct\text{-DNA}}$: 0, 0.56, 0.78, 1.09, 1.39, 1.88, 2.35, 2.80, 3.64, 4.41, 5.13, 6.40, 7.50, 8.46, 9.31, 10.06, 10.74 ($\times 10^{-4}$) M, from highest curve to lowest)

unchanged. Stern-Volmer equation was used to analyze the data of the fluorescence titrations of TAH with *ct*-DNA at two different temperatures (1) to reveal the quenching nature between *ct*-DNA and the derivative [26];

$$F_0/F = 1 + K_{sv}\,[Q] \quad (1)$$

F_0 and F represents the steady-state fluorescence intensities of TAH absence and presence of the *ct*-DNA, respectively. *ct*-DNA is the quencher and [Q] refers to the concentration of quencher. K_{sv} indicates the Stern–Volmer quenching constant. Figure 2 represents the linear Stern-Volmer plots obtained from fluorimetric titrations. K_{sv} values were evaluated from the slopes of the graphs for the interaction of TAH with *ct*-DNA. The results revealed that the K_{sv} values decreased with increase in temperature, suggests that the probable fluorescence quenching mechanisms of the compound by *ct*-DNA was static quenching. The obtained Stern-Volmer quenching constants from graphs are shown in Table 1.

The double logarithm regression curve which is evaluated from plot of $\log(F_0–F)/F$ versus $\log[Q]$ was used to calculate the binding constants. Following equation was used to plot graphs [27];

$$\log\,(F_0 - F)/F = \log K + n\,\log[Q] \quad (2)$$

where the binding constant K, and the binding site number n which can be determined from the slope of double logarithm regression curve. Figure 2 shows the double logarithm regression curve of the TAH-*ct*-DNA system. The obtained K and n values of TAH-*ct*-DNA system at various temperatures are represented in Table 1. Binding constants showed little increase by increase in temperature but they were still at the same order of magnitude. This result can be interpreted as the complex stability increases with the temperature.

Table 1 TAH-*ct*-DNA complex interaction parameters; quenching constants (K_{SV}), binding site numbers (n) and binding constants (K) values at two different tempretures

T (°C)	TAH		
	$K_{sv} \times 10^3$ (M^{-1})	K	n
298	2.299	1.92×10^2	0.629
310	1.522	4.21×10^2	0.819

Heavy Atom Effect on Binding

Iodide ion is one of the efficient quenchers for fluorescence systems. The molecules bound to the DNA surface like groove binders will be accessible to quencher when it is compared with intercalators. When small molecules intercalate into DNA, the molecule will be protected from the accessibility of the quencher by the close base pairs to the intercalator. In the case of intercalation also formed electrostatic repulsion between phosphate backbone of DNA and negatively charged quenchers will strengthen the shielding of the intercalated species [28].

A series of studies were performed to determine the accessibility of iodide ion to fluorescent probes by adding KI solution into TAH-*ct*-DNA system. The fluorescence spectra and the quenching curve for TAH-*ct*-DNA system were shown in Fig. 3. Gradual decrease in fluorescence intensity of the system was observed with increase in the iodide amount in the medium. This results reveals that the TAH binds to *ct*-DNA by groove binding.

Ionic Strength Effect on Binding

To assess the contribution of electrostatic forces in the interaction of DNA with DNA-binding molecules, investigation of

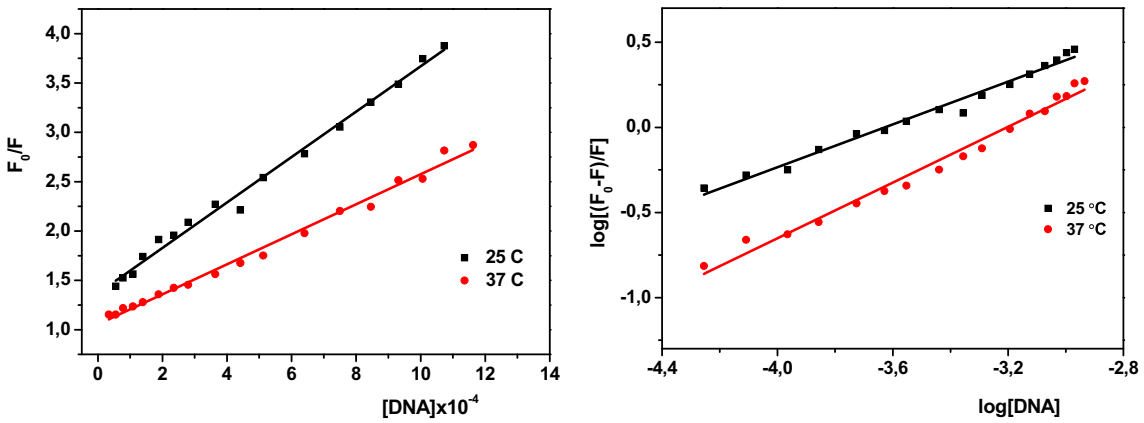

Fig. 2 The Stern-Volmer (left) and double-log plots (right) of *ct*-DNA quenching effect on TAH fluorescence at different temperatures

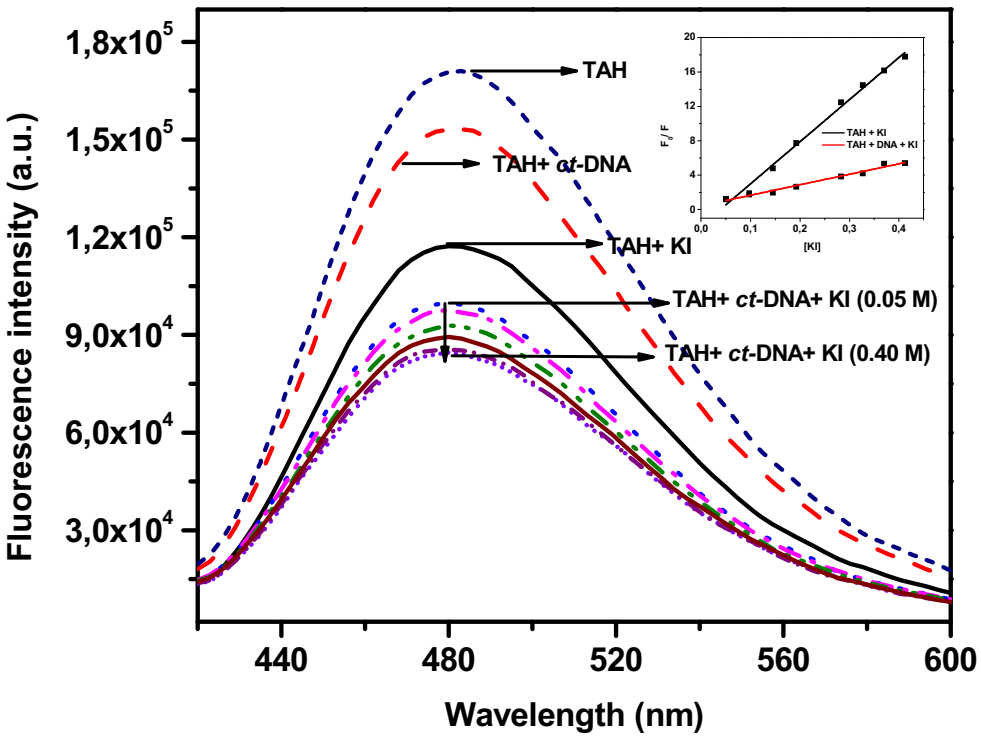

Fig. 3 Fluorescence emission spectra of TAH-*ct*-DNA system in the presence of KI. The Stern Volmer plots of KI quenching effect on free TAH and TAH-*ct*-DNA complex system is shown as inset graph

the effect of ionic strength on the system is necessary. It is a known fact that the electrostatic repulsion between negatively charged phosphate skeletons on adjacent nucleotides is decreased with increasing ionic strength. This characteristic causes the tightening the DNA chains, which makes the harder the interaction of organic molecules with nucleotide in DNA helix. The effect of NaCl on the fluorescence intensities of TAH-*ct*-DNA complex system was investigated (Fig. 4). The addition of NaCl to the free probe TAH, in the absence of DNA, didn't cause any remarkable change in the fluorescence properties of the probe. However, in the presence of *ct*-DNA, increase in salt concentration caused the increase in fluorescence intensities of the system. This is probably attributed to the release of the bound TAH from the *ct*-DNA

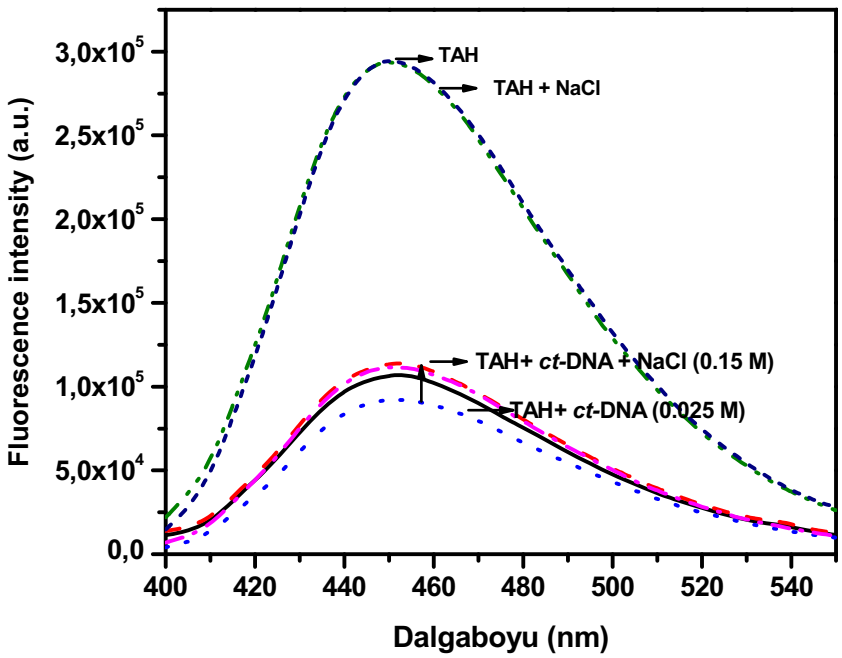

Fig. 4 Ionic strength effect on fluorescence spectra of free TAH and TAH-*ct*-DNA complex system

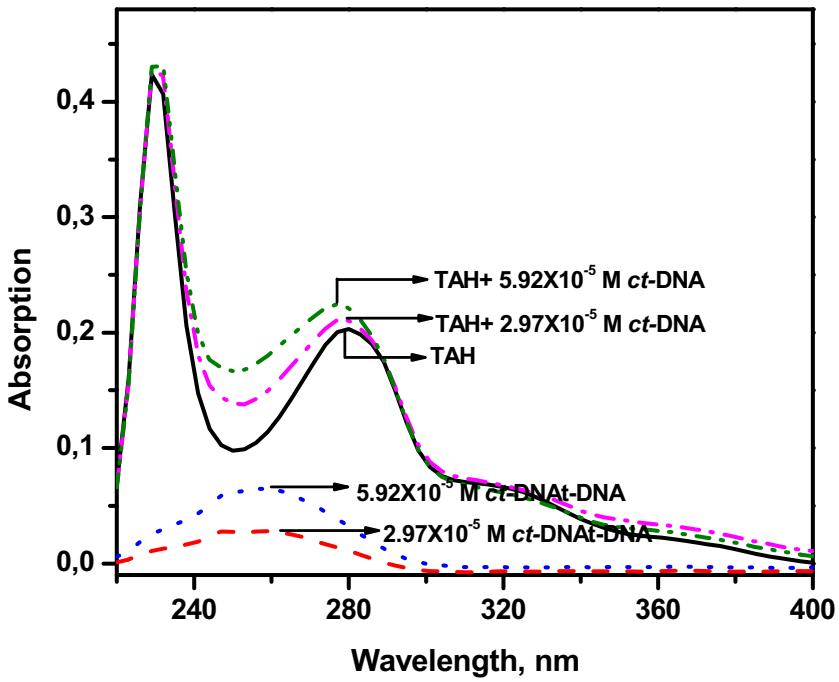

Fig. 5 UV-vis absorption spcetra of TAH in the absence and presence of *ct*-DNA ($2.97X10^{-5}$, $5.92X10^{-5}$ M) in 2 ml Tris-HCl buffer (pH = 8.0)

grooves into the solution [29]. The strong dependence of the binding on the ionic strength clearly indicates that TAH binding to *ct*-DNA is predominantly controlled by electrostatic interactions and this observation is consistent with groove binding.

UV-Vis Spectrum in the Presence of *ct*-DNA

Effect of DNA on the fluorescence intensities of the fluorophores gives remarkable information in DNA binding studies of small molecules. The absorption spectra of TAH in the absence and presence of different concentrations of *ct*-DNA were investigated. The absorption spectra of TAH have two distinct absorption bands around 230 nm and 280 nm. It is believed that these two bands are caused by the core structure of compounds. And the absorption spectra of the compound also have two small absorption bands around 320 and 360 nm. Intercalation commonly results in hypochromic and bathochromic effect while hyperchromic effect and a spectral shift accompanies to the groove binding [30]. The addition of *ct*-DNA to the TAH solution was resulted in increase of absorption amount of the complex systems. Effect of *ct*-DNA on absorption spectra of TAH is shown in Fig. 5. Despite the hyperchromocity of the bands, absorption maxima and the shape of the bands remained unchanged. The behavior of the system supports the idea that the TAH may bind to *ct*-DNA by groove binding.

Thermodynamic Studies on Binding of TAH with *ct*-DNA

Hydrophobic forces, van der Waals forces, electrostatic interactions, hydrogen bonds and covalent bonds are the primary forces between small molecules and targets. The thermodynamic parameters (ΔH, ΔG and ΔS) of the investigated system at two temperatures can be obtained by following thermodynamic Eqs. (3, 4).

$$\ln K_2/K_1 = -\Delta H/R\,[1/T_2 - 1/T_1] \quad (3)$$

$$\Delta G = \Delta H - T\,\Delta S = -R\,T\ln K \quad (4)$$

K_1 and K_2 are binding constants of TAH-*ct*-DNA complex system at 25 and 37 °C, individually. The characteristic signs of the thermodynamic parameters in

Table 2 Thermodynamic analysis results and the interaction type of the complex system

Derivative	ΔH (kJ/mol)	TΔS (K.kJ/mol)	ΔG (kJ/mol)	Interaction mode
TAH	50.59	63.61	−13.03	Hydrophobic forces

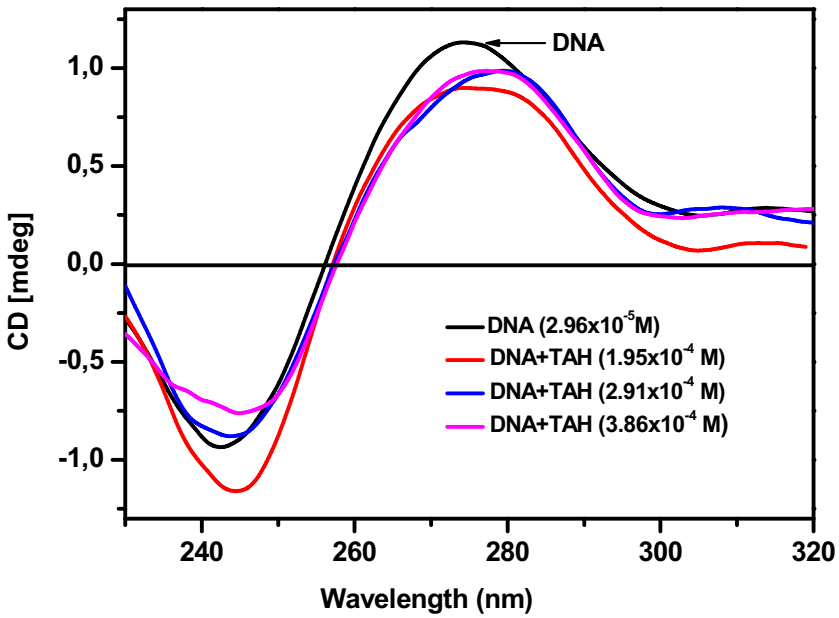

Fig. 6 Circular dichroism spectrum of *ct*-DNA in absence and presence of different concentration of TAH at 298 K

protein association processes suggest the driving forces in the interaction of small molecules with targets [27, 31]. Studies revealed that;

$\Delta H < 0$ or $\Delta H \approx 0$ and $\Delta S > 0$: The main acting force is electrostatic force as main acting force
$\Delta H < 0$ and $\Delta S < 0$: The main acting force is van der Waals or hydrogen bond
$\Delta H > 0$ and $\Delta S > 0$: The main force is hydrophobic forces
$\Delta H < 0$ or $\Delta S \approx 0$ and $\Delta S > 0$: The main acting force is ionic

Thermodynamic results of the investigated interactions were obtained and listed in Table 2. Positive values of ΔH and ΔS mark the hydrophobic interactions in the binding mechanism of TAH to *ct*-DNA. The negative value of ΔG reveals the spontaneous interaction between probe and *ct*-DNA [32].

Circular Dichroism (CD) Spectroscopy

CD is one of the techniques to follow the conformational changes in the secondary structure of the *ds*-DNA helix. The CD spectrum of free *ds*-DNA exhibits a positive band at 275 nm due to base stacking and negative band at around 248 nm due to polynucleotide helicity [33]. Both of these bands are highly sensitive to *ds*-DNA interaction with small molecules. An increase in the positivity of the band at 275 nm is one of the characteristics of the intercalative binding as a result of the stacking interaction of the intercalator between the base pairs of *ds*- DNA [34]. Despite that groove binders generally don't cause any significant unwinding of the *ds*-DNA base pairs. The CD spectra of free *ct*-DNA and its complex with different TAH concentrations are shown in Fig. 6. A decrease in intensity of positive band was observed and slight increase in intensity of negative band was examined upon addition of TAH indicating that possible mechanism of interactions of derivative with *ct*-DNA is groove binding.

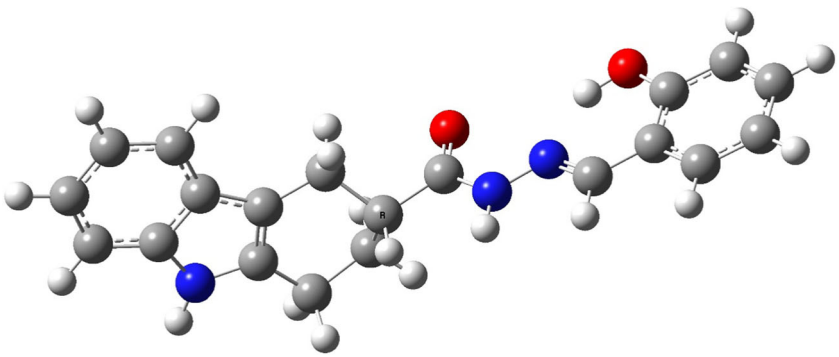

Fig. 7 The geometry optimized compound TAH at DFT/ B3LYP/ 6-31G* basis set in Gaussian09

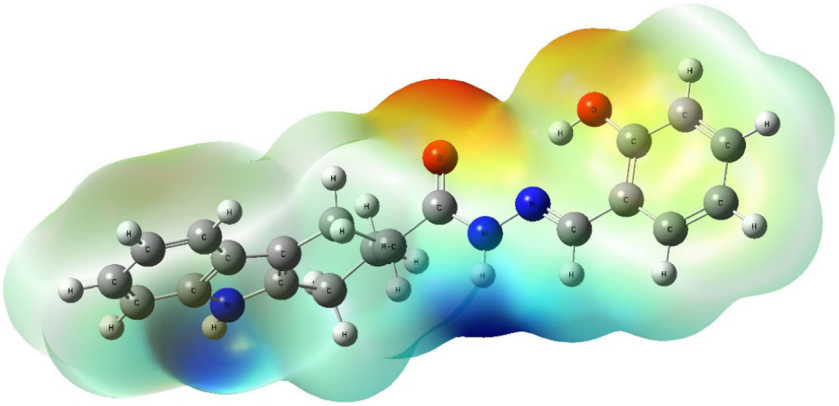

Fig. 8 Molecular electrostatic potential map of TAH

Computational Results

Figure 7 shows the optimized structure of TAH in this study. Additional information of the compound was given at TS1 in supporting information part. Furthermore, molecular electrostatic potential surface (MEPS) was computed to probe reactive sites of electrophilic and nucleophilic attacks of TAH.

The MESP map in the case of TAH shown the potential distribution between carbonyl oxygen and hydroxyl oxygen atoms (dark red) and nitrogen atoms of hidrazide and carbazole moeities (dark blue) and represented in Fig. 8. Based on the MEPS, it was revealed that the negative charge covered the carbonyl and hydroxyl oxygen groups and the positive region was over the nitrogen atom of the hidrazide and carbazole groups. The most reactive part in TAH is the carbonyl oxygen of hidrazide group due to its electronegativity.

Docking Results

The molecular docking process were applied for understanding interactions between the entitled compound and DNAs.

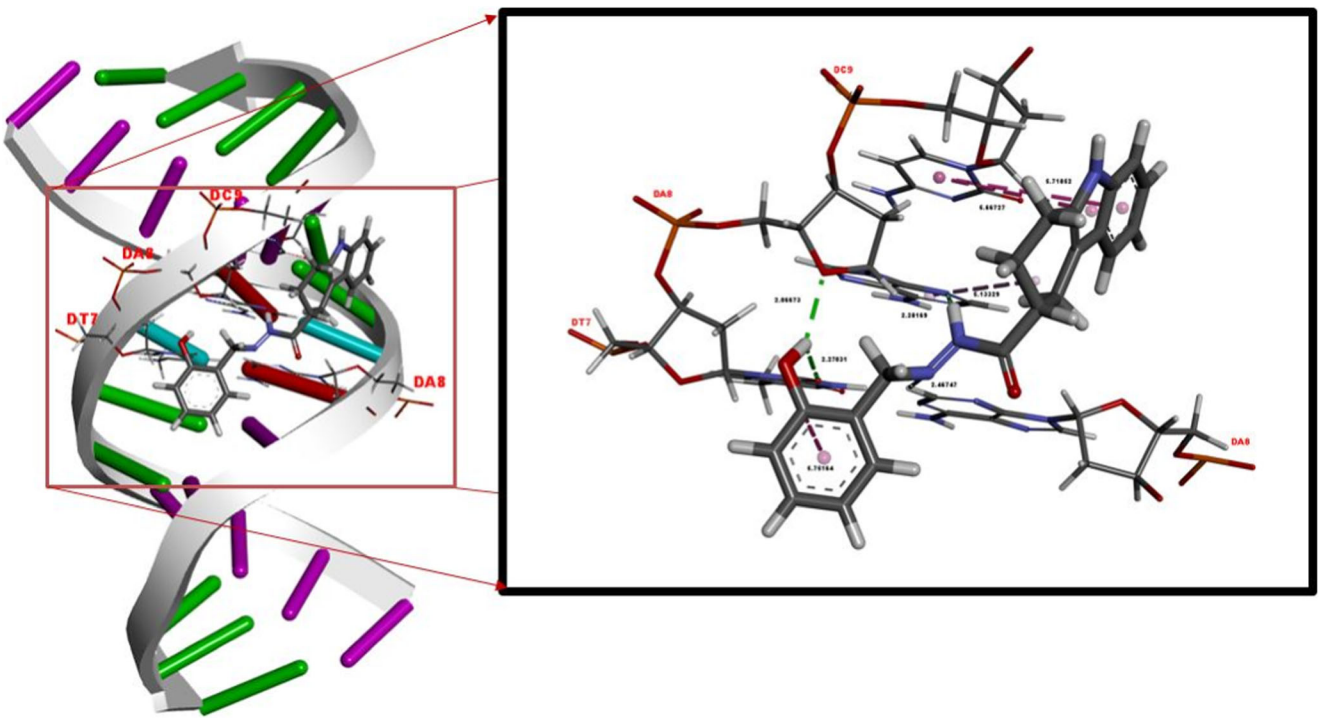

Fig. 9 Docking poses and interactions of compound TAH in A_DNA

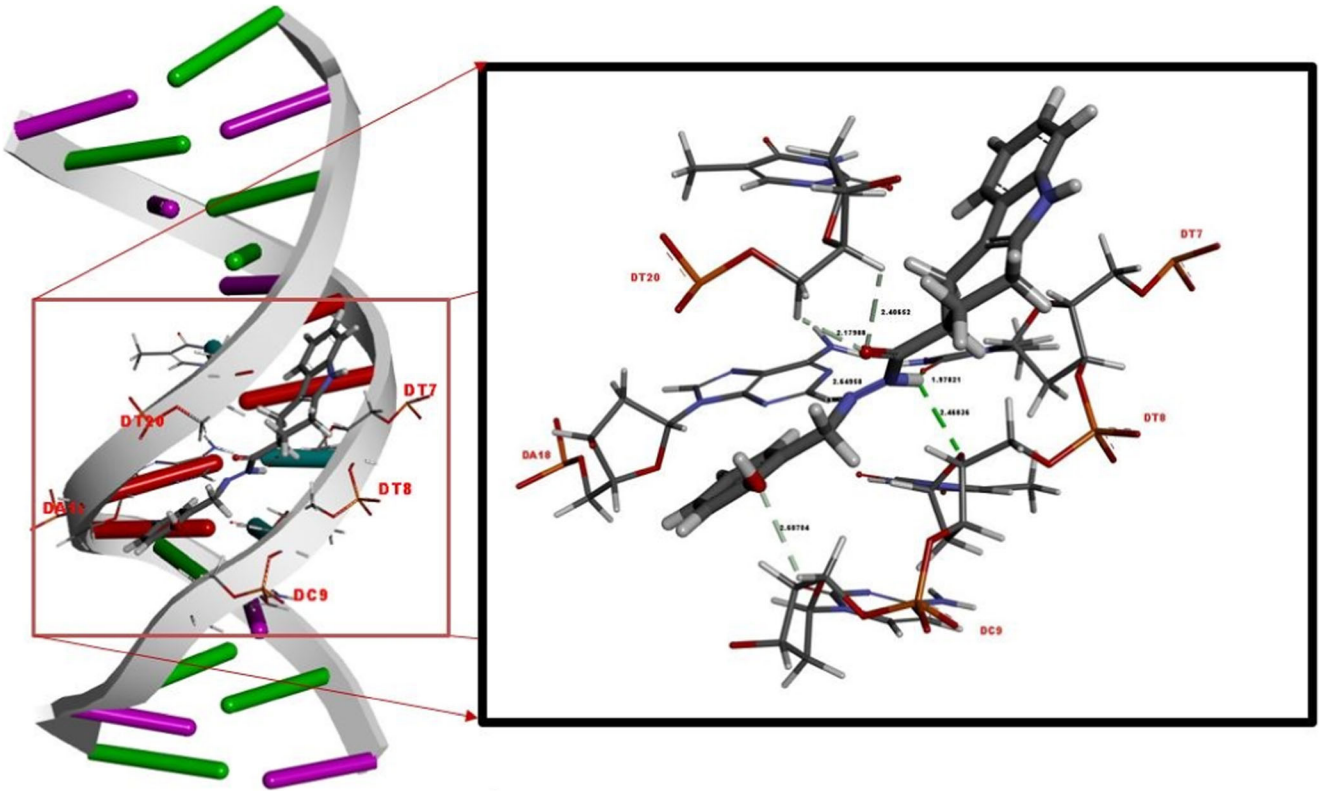

Fig. 10 Docking poses and interactions of compound TAH in B_DNA

The docked TAH-A_DNA complex and its three dimensional interactions are given in Fig. 9. This complex has three hydrogen bonds and four hydrophobic interactions with active nucleotides B:DT7, B:DA8 and B:DC9. On the other hand, Fig. 10 presented that TAH has six hydrogen bonds with active nucleotides A:DT7, A:DT8, A:DC9 and B:DA18, B:DT20 of B_DNA. Additionally, binding energy and Ki values for each complex were computed and displayed in Table 3. According to the results of the experiment, TAH-A_DNA complex results are more appropriate when compared to TAH-B_DNA complex results. In summary, the results of docking show that hydrophobic interactions are more effective than hydrogen bonds. In addition, interaction types and distances for the TAH compound against each DNA isomer were confirmed at TS2 in supporting information section.

Table 3 Binding energy and inhibition constant (Ki) values of the generated complexes

Complex	ΔG(kJ/mol)	Ki (nM)
TAH-A_DNA	−35.19	688.37
TAH-B_DNA	−44.18	18.11

Conclusions

The effect of *ct*-DNA on a tetrahydrocarbazole derivative was examined by various spectral methods. The results show that the static quenching process is the main quenching mechanism in the TAH-*ct*-DNA complex system. The binding reaction of TAH with *ct*-DNA is spontaneous. Thermodynamic parameters deduce the hydrophobic interactions (positive ΔH and positive ΔS) is driven force in the TAH-*ct*-DNA complex. Results of the heavy atom effect and ionic strength effect on fluorescence intensity of the TAH-*ct*-DNA complex indicate the groove binding between *ct*-DNA and derivative. UV-vis absorption studies and CD results also support the groove binding suggestion. Moreover, computational results with docking types and interactions with DNA supports the experimental results. Additionaly, computational studies exhibit why TAH compound is promising structure based on the MEPS map and A_DNA isomer has more compatible interaction with TAH compound based on the docking and experimental results. This research has significance to get different sights of pharmacological and medicinal applications the probability of using tetrahydrocarbazole derivatives.

Acknowledgements This work was supported by the Scientific and Technical Research Council of Turkey (TUBITAK) - Grant No 114Z391.

References

1. Ramana MMV, Betkar R, Nimkar A, Ranade P, Mundhe B, Pardeshi S (2016) Synthesis of a novel 4H-pyran analog as minor groove binder to DNA using ethidium bromide as fluorescence probe. Spectrochim Acta Part A 152:165–171
2. Singh MP, Joseph T, Kumar S, Bathini Y, Lown JW (1992) Synthesis and sequence-specific DNA binding of a topoisomerase inhibitory analog of Hoechst 33258 designed for altered base and sequence recognition. Chem Res Toxicol 5:597–607
3. Sparks J, Scholz C (2009) Evaluation of a cationic Poly(β-hydroxyalkanoate) as a plasmid DNA delivery system. Biomacromolecules 10:1715–1719
4. Lown JW (1998) Anticancer Drug Des 3:25–40
5. Gurova K (2009) New hopes from old drugs: revisiting DNA-binding small molecules as anticancer agents. Future Oncol 5: 1685–1704
6. Boer DR, Canals A, Coll M (2009) Dalton Trans 3:399–414
7. Pindur U, Jansen M, Lemster T (2005) Advances in DNA-ligands with groove binding, intercalating and/or alkylating activity: chemistry, DNA-binding and biology. Curr Med Chem 12:2805–2847
8. Strekowski L, Wilson B (2007) 623: 3–13
9. Li J, Li B, Wua Y, Shuang S, Dong C, Choi MMF (2012) Luminescence and binding properties of two isoquinoline alkaloids chelerythrine and sanguinarine with ctDNA. Spectrochim Acta Part A 95:80–85
10. Temerk Y, Ibrahim M, Ibrahim H, Kotb M (2015) Interactions of an anticancer drug Formestane with single and double stranded DNA at physiological conditions. J Photochem Photobiol B 149:27–36
11. Knolker HJ, Reddy KR (2002) Isolation and synthesis of biologically active carbazole alkaloids. Chem Rev 102:4303–4427
12. Sultan A, Sulthana SS, Kamil SRM, Shafi SS (2009) Indian J Heterocycl Chem 18:385–388
13. Gudmundsson KS, Sebahar PR, Richardson LD, Catalano JG, Boggs SD, Spaltenstein A, Sethna PB, Brown KW, Harvey R, Romines KR (2009) Substituted tetrahydrocarbazoles with potent activity against human papillomaviruses. Bioorg Med Chem Lett 19:3489–3492
14. Chen J, Lou J, Liu T, Wu R, Dong X, He Q, Yang B, Hu Y (2009) Synthesis and in-vitroantitumor activities of some mannich bases of 9-Alkyl-1,2,3,4-tetrahydrocarbazole-1-ones. Arch Pharm Chem Life Sci 342:165–172
15. Vicini P, Zani F, Cozzini P, Doytchinova I (2002) Hydrazones of 1, 2-benzisothiazole hydrazides: synthesis, antimicrobial activity and QSAR investigations. Eur J Med Chem 37:553–564
16. Popp FD (1989) Potential anticonvulsant. XII. Anticonvulsant activity of some aldehyde derivatives. Eur J Med Chem 24:313–315
17. Todeschini AR, de Miranda ALP, da Silva KCM, Parrini SC, Barreiro EJ (1998) Synthesis and evaluation of analgesic, antiinflammatory and antiplatelet properties of new 2-pyridylarylhydrazone derivatives. Eur J Med Chem 33:189–199
18. Melnyk P, Leroux V, Sergheraert C, Grellier P (2006) Design, synthesis and in vitro antimalarial activity of an acylhydrazone library. Bioorg Med Chem Lett 16:31–35
19. Kocyigit KB, Rollas S (2002) Synthesis, characterization and evaluation of antituberculosis activity of some hydrazones. Farmaco 57: 595–599
20. Morris GM, Huey R, Lindstrom W, Sanner MF, Belew RK, Goodsell DS, Olson AJ (2009) Autodock4 and AutoDockTools4: automated docking with selective receptor flexiblity. J Comput Chem 16:2785–2791
21. Mandal PK, Venkadesh S, Gautham N (2012) Structure of the tetradecanucleotide d (CCCCGGTACCGGGG)2 as an A-DNA duplex. Acta Crystallogr Sect F: Struct Biol Cryst Commun 68:393–399
22. Drew HR, Wing RM, Takano T, Broka C, Tanaka S, Itakura K, Dikerson RE (1981) Structure of a B-DNA dodecamer: conformation and dynamics. Proc Natl Acad Sci U S A 78:2179–2183
23. Gaussian09, RevisionE.01, Frisch MJ, Trucks GW, Schlegel HB, Scuseria GE, Robb MA, Cheeseman JR, Scalmani G, Barone V, Mennucci B, Petersson GA, et al. (2009). Gaussian, Inc., Wallingford, CT
24. Chattaraj PK, Giri S, Duley S (2011) Chem Rev 111:43–75
25. Dassault Systemes Biovia (2016) Discovery studio modeling environment release 2017. Dassault Systemes, San Diego
26. Lakowicz JR (2006) 3rd edn. Springer, New York
27. Sun Y, Bi S, Song D, Qiao C, Mu D, Zhang H (2008) Study on the interaction mechanism between DNA and the main active components in Scutellaria baicalensis Georgi. Sensors Actuators B Chem 129:799–810
28. Qui B, Guo L, Wang W, Chen G (2007) Biosens Bioelectron 22: 2629–2635
29. Kumar CV, Turner RS, Asuncion EH, Photochem J (1993) Groove binding of a styrylcyanine dye to the DNA double helix: the salt effect. Photobiol A Chem 74:231–238
30. Wu M, Wu W, Lian X, Lin X, Xie Z (2008) Synthesis of a novel fluorescent probe and investigation on its interaction with nucleic acid and analytical application. Spectrochim Acta Part A 71:1333–1340
31. Ross PD, Subramanian S (1981) Thermodynamics of protein association reactions: forces contributing to stability. Biochemistry 20: 3096–3102
32. Bi S, Yan L, Sun Y, Zhang H (2011) Investigation of ketoprofen binding to human serum albumin by spectral methods. Spectrochim Acta Part A 78:410–414
33. Maheswari PU, Palaniandavar M (2004) DNA binding and cleavage properties of certain tetrammine ruthenium(II) complexes of modified 1,10-phenanthrolines – effect of hydrogen-bonding on DNA-binding affinity. J Inorg Biochem 98:219–230
34. Garbett NC, Ragazzon PA, Charires JB (2007) Nat Protoc 12:3166–3172